

Btn2a2, a T cell immunomodulatory molecule coregulated with MHC class II genes

Kerstin Sarter,¹ Elisa Leimgruber,¹ Florian Gobet,¹ Vishal Agrawal,¹ Isabelle Dunand-Sauthier,¹ Emmanuèle Barras,¹ Béatrix Mastelic-Gavillet,^{1,2} Arun Kamath,^{1,2} Paola Fontannaz,^{1,2} Leslie Guéry,¹ Fernanda Do Valle Duraes,¹ Carla Lippens,¹ Ulla Ravn,³ Marie-Laure Santiago-Raber,¹ Giovanni Magistrelli,³ Nicolas Fischer,³ Claire-Anne Siegrist,^{1,2} Stéphanie Hugues,¹ and Walter Reith¹

¹Department of Pathology and Immunology, Faculty of Medicine and ²Department of Pediatrics, World Health Organization Collaborating Center for Vaccinology and Neonatal Immunology, University of Geneva, 1211 Geneva, Switzerland

³Novimmune SA, 1228 Plan-les-Ouates, Switzerland

Evidence has recently emerged that butyrophilins, which are members of the extended B7 family of co-stimulatory molecules, have diverse functions in the immune system. We found that the human and mouse genes encoding butyrophilin-2A2 (BTN2A2) are regulated by the class II trans-activator and regulatory factor X, two transcription factors dedicated to major histocompatibility complex class II expression, suggesting a role in T cell immunity. To address this, we generated *Btn2a2*-deficient mice. *Btn2a2*^{-/-} mice exhibited enhanced effector CD4⁺ and CD8⁺ T cell responses, impaired CD4⁺ regulatory T cell induction, potentiated antitumor responses, and exacerbated experimental autoimmune encephalomyelitis. Altered immune responses were attributed to *Btn2a2* deficiency in antigen-presenting cells rather than T cells or nonhematopoietic cells. These results provide the first genetic evidence that BTN2A2 is a co-inhibitory molecule that modulates T cell-mediated immunity.

Butyrophilins constitute a family of transmembrane proteins comprising butyrophilin (BTN), BTN-like (BTNL), and selection and upkeep of intraepithelial T cell (SKINT) proteins (Arnett and Viney, 2014). Their extracellular moieties contain IgV and IgC2 domains exhibiting homology to the corresponding domains of B7 co-stimulatory molecules (Arnett and Viney, 2014), and butyrophilins are thus considered to be members of the extended B7 family.

As a result of gene duplications and deletions, alterations in domain structure, and loss of gene function, the butyrophilin family exhibits major divergences between species (Afrache et al., 2012). Only five butyrophilin genes—*BTN1A1/Btn1a1*, *BTN2A/Btn2a2*, *BTNL2/Btnl2*, *BTNL9/Btnl9*, and *BTNL10/Btnl10*—are conserved between humans and mice. Many human (*BTNL2* and BTNs) and mouse (*Btn1a1*, *Btn2a2*, *Btnl2*, and *Btnl4–7*) genes are located in the MHC (Afrache et al., 2012).

BTN1A1, the first butyrophilin identified, is required for the formation, secretion, and stabilization of milk fat globules (Ogg et al., 2004). Growing evidence subsequently suggested that butyrophilins play diverse roles in the immune

system. Functions have been best elucidated for mouse SKINT1 and human *BTN3A1*, which are not among the conserved family members. SKINT1 drives the thymic differentiation of mouse V γ 5⁺V δ 1⁺ T cells (Boyden et al., 2008). Activation of human V γ 9⁺V δ 2⁺ T cells by phosphoantigens is mediated by *BTN3A1* (Vavassori et al., 2013; Sandstrom et al., 2014). Knowledge of the functions of other butyrophilins remains fragmentary. Polymorphisms in *BTNL2* were linked with various autoimmune and inflammatory diseases (Arnett and Viney, 2014). The MHC region encompassing BTN genes was linked to type 1 diabetes (Viken et al., 2009). In vitro experiments revealed that antibodies (Ab's) against human *BTN3* proteins can either inhibit T cell activation or promote activation of T cells, monocytes, and DCs (Arnett and Viney, 2014). Mouse *BTNL2* is expressed by epithelial cells and DCs in the small intestine and Peyer's patches, where it is up-regulated during intestinal inflammation (Arnett et al., 2007). Blocking Ab's against *BTNL1* enhance T cell responses in vivo and exacerbate experimental autoimmune encephalomyelitis (EAE) and asthma in mouse models (Yamazaki et al., 2010). *BTNL1*-Fc, *BTNL2*-Fc, *BTN1A1*-Fc, and *BTN2A2*-Fc fusion proteins inhibit T cell activation, proliferation, and cytokine production in vitro (Arnett et al., 2007; Smith et al., 2010; Ammann et al., 2013; Swanson et al., 2013). *BTNL2*-Fc and *BTN2A2*-Fc also induce *Foxp3* expression and T_{reg} differentiation in vitro (Ammann et al., 2013; Swanson et al., 2013). Lastly, staining with butyrophil-

Correspondence to Walter Reith: walter.reith@unige.ch

E. Leimgruber's present address is MyCartis, Ecole Polytechnique Federale de Lausanne, 1015 Lausanne, Switzerland.

M.-L. Santiago-Raber's present address is Tolerys SA, 1205 Geneva, Switzerland.

Abbreviations used: Ab, antibody; BTN, butyrophilin; BTNL, BTN-like; ChIP, chromatin immunoprecipitation; CIITA, class II trans-activator; dLN, draining LN; EAE, experimental autoimmune encephalomyelitis; ES, embryonic stem; MOG, myelin oligodendrocyte glycoprotein; qRT-PCR, quantitative RT-PCR; RFX, regulatory factor X; RT, room temperature; SC, spinal cord; SKINT, selection and upkeep of intraepithelial T cell.

© 2016 Sarter et al. This article is distributed under the terms of an Attribution-Noncommercial-Share Alike-No Mirror Sites license for the first six months after the publication date (see <http://www.rupress.org/terms>). After six months it is available under a Creative Commons License (Attribution-Noncommercial-Share Alike 3.0 Unported license, as described at <http://creativecommons.org/licenses/by-nc-sa/3.0/>).

in-Fc reagents has suggested the presence of unidentified receptors on T cells (Smith et al., 2010; Arnett and Viney, 2014).

We recently discovered that human *BTN2A2* and mouse *Btn2a2* are regulated by the class II trans-activator (CIITA) and regulatory factor X (RFX), two transcription factors dedicated to MHC class II (MHCII) expression (Reith et al., 2005), suggesting a role in APCs. To address this question, we generated and analyzed *Btn2a2*^{-/-} mice. Results confirmed that *BTN2A2* expression by APCs modulates T cell responses.

RESULTS AND DISCUSSION

Regulation of *BTN2A2* expression by RFX and CIITA

MHCII promoters contain a characteristic enhancer—the SXY module—controlled by well-defined transcription factors comprising CIITA and RFX (Fig. 1 A; Reith et al., 2005). The conserved architecture of the SXY module allowed the design of a stringent sequence profile that was used to scan the human genome for similar enhancers (Krawczyk et al., 2007). A strong SXY homology was found in the *BTN2A2* promoter (Fig. 1 B). This SXY module is conserved in orthologous genes of other species, including mouse *Btn2a2* (Fig. 1 C).

Binding of CIITA to the *BTN2A2* promoter was observed, albeit with low confidence, in chromatin immunoprecipitation (ChIP)—on-microarray experiments (Krawczyk et al., 2008). ChIP assays confirmed that both CIITA and RFX are recruited to the *BTN2A2* promoter in B cells (Fig. 1 D). As the binding of CIITA is dependent on RFX, its recruitment is abolished in RFX-deficient cells. Binding of RFX is destabilized in CIITA-deficient cells. CIITA and RFX binding was also induced by IFN- γ . Patterns of RFX and CIITA binding at the *BTN2A2* promoter closely matched those observed at the *HLA-DRA* promoter.

Human *BTN2A2* mRNA expression was strongly reduced in CIITA- and RFX-deficient B cells (Fig. 1 E). *BTN2A2* expression in CIITA-deficient cells was restored by complementation with CIITA (Fig. 1 E). IFN- γ -induced *BTN2A2* expression was also aborted in CIITA-deficient cells (Fig. 1 E). The dependence of *BTN2A2* expression on RFX and CIITA was identical to that of *HLA-DRA*.

Mouse *Btn2a2* mRNA expression was abrogated in B cells from *CIITA*^{-/-} and *Rfx5*^{-/-} mice, BMDCs from *CIITA*^{-/-} mice, and IFN- γ -induced embryonic fibroblasts from *CIITA*^{-/-} mice (Fig. 1 F). The dependence of *Btn2a2* mRNA expression on RFX and CIITA was identical to that of *H2-Aa*. *BTN2A2* protein expression was also abolished in *Rfx5*^{-/-} and *CIITA*^{-/-} B cells, confirming the regulation by RFX and CIITA (Fig. 1 G). The regulation of mouse *Btn2a2* by CIITA and RFX is consistent with expression by APCs (B cells and DCs), IFN- γ -induced cells, and thymic epithelial cells (not depicted; Smith et al., 2010).

Reporter assays demonstrated that activation of the *BTN2A2* promoter by RFX and CIITA is conferred by the SXY module: constructs driven by the *HLA-DRA* promoter, the *BTN2A2* promoter, and a hybrid *HLA-DRA* promoter

containing the SXY module of *BTN2A2* exhibited similar dependencies on CIITA and RFX (Fig. 1 H). Mutation analysis indicated that activity of the *BTN2A2* SXY module depends mainly on the X element and, to a lesser extent, the Y element (Fig. 1 I), which are the two most conserved sequences (Fig. 1 C). Mutations in S and X2 had no adverse effects (Fig. 1 I). This is similar to MHCII promoters, where mutations in X and Y typically impair activity more than those in S and X2.

Generation of *Btn2a2*^{-/-} mice

Btn2a2^{-/-} mice (Fig. 2 A) are viable, fertile, and exhibit no overt developmental defects. Histological examinations revealed no abnormalities in 8-wk-old mice (not depicted). Flow cytometry analyses revealed no significant alterations in steady-state populations of CD19⁺ B cells, CD3⁺ T cells, CD4⁺ and CD8⁺ T cells, $\gamma\delta$ T cells, NK and NKT cells, plasmacytoid and conventional DCs, LN-resident CD8⁻ and CD8⁺ DCs, migratory DCs, or double-negative, double-positive, and single-positive thymocytes (not depicted).

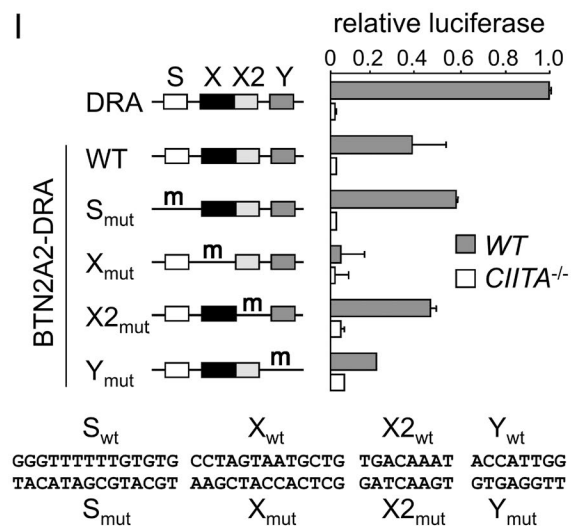
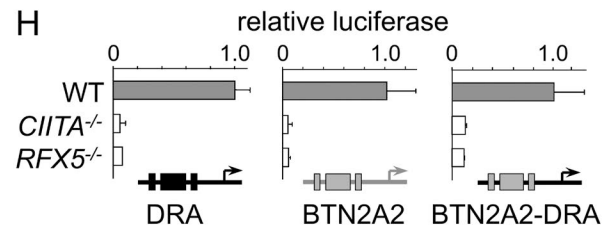
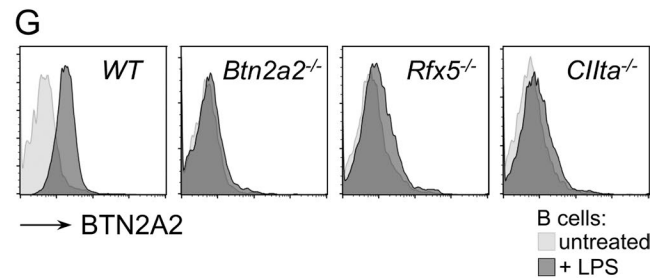
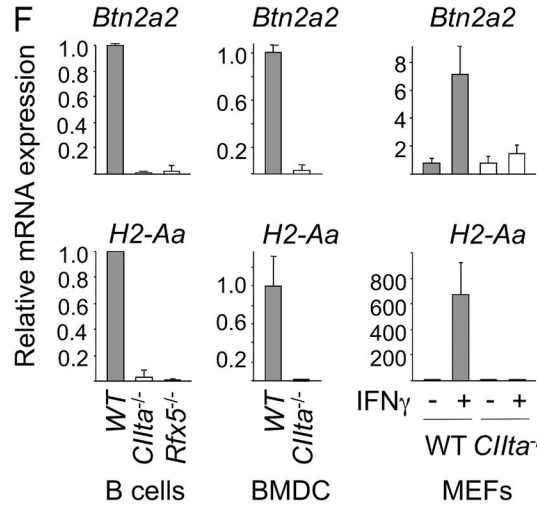
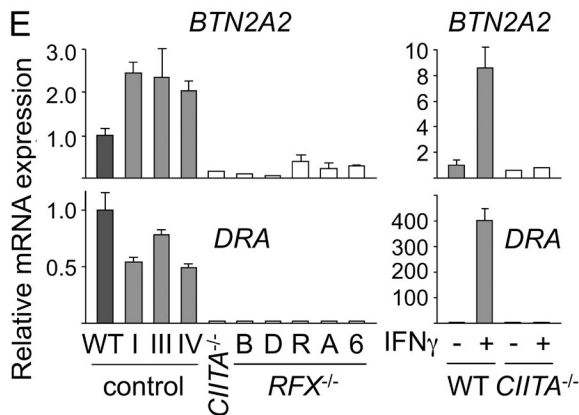
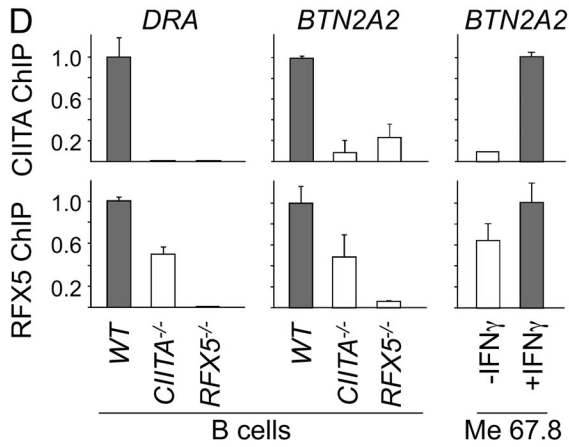
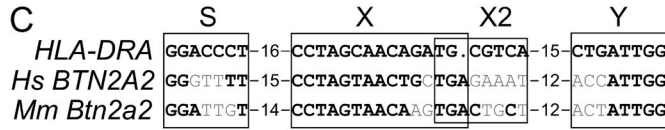
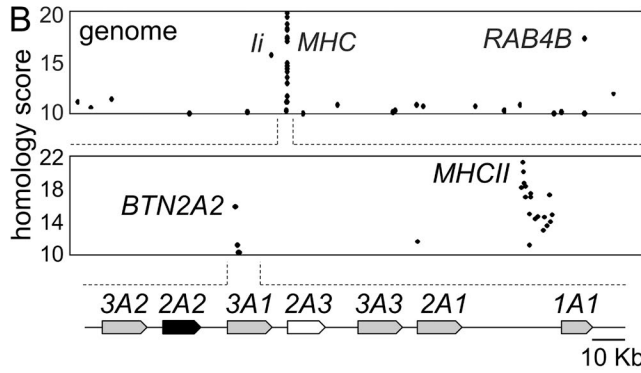
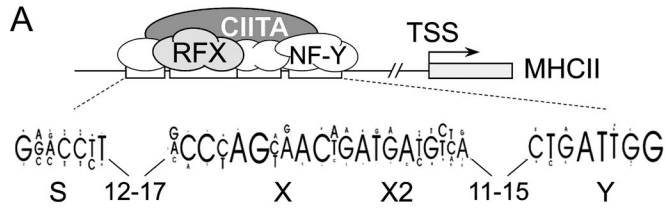
Btn2a2^{-/-} mice exhibit enhanced T cell responses

WT and *Btn2a2*^{-/-} mice were immunized with OVA using adjuvants that favor Th2 (alum) or Th1 (alum + CpG) responses. In the Th1 setting, *Btn2a2*^{-/-} mice developed increased numbers of OVA-specific IFN- γ ⁺ T cells, and these cells produced more IFN- γ after in vitro restimulation (Fig. 2 B). Conversely, *Btn2a2*^{-/-} mice immunized under Th2 conditions developed increased numbers of OVA-specific IL-5⁺ T cells, and these cells produced more IL-5 after in vitro restimulation (Fig. 2 B). No differences between *Btn2a2*^{-/-} and WT T cells were evident for TGF- β , IL-6, or TNF production (Fig. 2 B). Serum titers of OVA-specific IgG, IgG1, and IgG2c Ab's induced by immunization under Th1 and Th2 conditions were consistently more elevated, albeit moderately, in *Btn2a2*^{-/-} mice (not depicted).

Btn2a2 expression by APCs regulates T cell responses

Irradiated WT mice reconstituted with *Btn2a2*^{-/-} BM (KO \rightarrow WT) and irradiated *Btn2a2*^{-/-} mice reconstituted with WT BM (WT \rightarrow KO) were immunized with OVA under Th1 conditions. The numbers of IFN- γ ⁺ T cells and frequencies of IFN- γ ⁺CD4⁺ T cells were more elevated, whereas the frequencies of Foxp3⁺CD4⁺ T_{reg} cells were reduced, in KO \rightarrow WT chimeras (Fig. 2 C).

OTII T cell transfer experiments performed with WT and *Btn2a2*^{-/-} mice indicated that altered T cell responses resulted from *Btn2a2* deficiency in APCs. Frequencies of proliferating and IFN- γ ⁺ OTII T cells were increased, whereas frequencies of Foxp3⁺ OTII T cells were decreased, in draining LNs (dLNs) of OVA-immunized *Btn2a2*^{-/-} mice (Fig. 2 D). This bias was OVA dependent, as it was not observed after administration of adjuvant alone and was less pronounced in non-draining LNs (Fig. 2 E). Furthermore, responses of co-transferred myelin oligodendrocyte glycoprotein (MOG)-specific 2D2 CD4⁺ T



cells were not altered (not depicted). Transfer experiments with OVA-specific T cells from OTI mice demonstrated that CD8⁺ T cell responses were also boosted in *Btn2a2*^{-/-} mice (Fig. 2 F).

These results indicate that *Btn2a2* deficiency in BM-derived APCs, rather than T cells, perturbs the balance between Th and T_{reg} responses. Contributions of BTN2A2 expression by different APCs remain to be defined. Furthermore, although the use of BM chimeras revealed a role of BTN2A2 expression by cells of hematopoietic origin, they do not exclude a role in nonhematopoietic cells. BTN2A2 is notably expressed in thymic epithelial cells and nonprofessional APCs induced with IFN- γ . Deciphering the respective roles of BTN2A2 expression by different cell types will require the use of mice exhibiting cell type-specific deletion of *Btn2a2*.

Direct modulation of T cell responses by BTN2A2

In vitro T cell activation assays were used to investigate whether BTN2A2 has a direct effect on T cells. WT T cells were activated with anti-CD3 Ab's in the presence or absence of a BTN2A2-Fc fusion protein. BTN2A2-Fc inhibited CD4⁺ T cell activation, proliferation, and IFN- γ production (Fig. 2, G and H). CD4⁺Foxp3⁺ T_{reg} cells were instead increased (Fig. 2 G). WT and *Btn2a2*^{-/-} CD4⁺ T cells responded similarly, indicating that BTN2A2 expression by T cells is not implicated (Fig. 2, G and H). The effects of BTN2A2-Fc on CD4⁺ T cells were not countered by co-stimulation with anti-CD28 (Fig. 2 G and not depicted). Activation of CD8⁺ T cells was also strongly impaired by BTN2A2-Fc (Fig. 2 I).

These findings imply that BTN2A2 exerts its immunomodulatory functions by binding to a receptor on T cells. This is consistent with the staining of T cells with BTN2A2-Fc proteins (Smith et al., 2010). A mechanistic understanding of the immunoregulatory functions of BTN2A2 will require molecular identification of its T cell receptors. Identifying butyrophilin receptors remains a major challenge. To date, coun-

terreceptors have been reported for only two butyrophilins. Human BTN3A1 can interact with the TCR of V γ 9V δ 2 T cells (Vavassori et al., 2013). DC-SIGN can bind to human BTN2A1, an interaction hypothesized to play a role in tumor immunosurveillance (Malcherek et al., 2007).

Autoimmune responses in *Btn2a2*^{-/-} mice

MOG-induced EAE experiments indicated that *Btn2a2*^{-/-} mice exhibited greater mean and maximum clinical scores as well as increased incidence during disease onset and peak disease (Fig. 3 A). EAE experiments with KO \rightarrow WT and WT \rightarrow KO chimeras confirmed that disease exacerbation was the result of *Btn2a2* deficiency in BM-derived cells: KO \rightarrow WT chimeras exhibited greater mean and maximum disease scores as well as increased incidence during disease onset (Fig. 3 A).

Exacerbated EAE in *Btn2a2*^{-/-} mice was associated with increased spinal cord (SC) infiltration by total CD4⁺ T cells and MOG-specific IFN- γ ⁺ and IL-17⁺CD4⁺ cells. Both increased frequencies (not depicted) and absolute numbers (Fig. 3 B) of infiltrating IFN- γ ⁺ and IL-17⁺CD4⁺ T cells were evident at disease onset and peak disease. The numbers of infiltrating Foxp3⁺ T_{reg} cells were increased during disease onset, although this was not evident at peak disease (Fig. 3 B) and not observed at the level of T_{reg} frequencies. Ratios between infiltrating Th and T_{reg} cells were strongly skewed in favor of pathogenic Th1 and Th17 cells (Fig. 3 C).

CD4⁺ T cell responses were also altered in dLNs of *Btn2a2*^{-/-} mice: increased frequencies of MOG-specific IFN- γ ⁺ and/or IL-17⁺CD4⁺ T cells were evident at disease onset and peak disease, whereas frequencies of proliferating Foxp3⁺ T_{reg} cells were reduced before disease onset (Fig. 3 D).

Young *Btn2a2*^{-/-} mice did not exhibit overt signs of spontaneous autoimmunity, such as tissue inflammation or increased serum titers of tissue-reactive Ab's. However, increased titers of anti-DNA Ab's were observed in 1-yr-old *Btn2a2*^{-/-} mice (Fig. 3 E), suggesting that a loss of self-tolerance may develop with age.

Figure 1. Coregulation of BTN2A2 with MHCII genes. (A) Schematic representation of transcription factors (RFX, NF-Y, and CIITA) bound to the SXY module of MHCII promoters. The consensus SXY sequence is shown. TSS, transcription start site. (B) The human genome was scanned for promoters containing SXY motifs. Homology scores are plotted as a function of position in the genome. Dots corresponding to known RFX and CIITA targets (*BTN2A2*, *RAB4B*, *li*, and MHCII genes) are labeled. A map of the BTN locus is indicated underneath the graphs. (C) Human *BTN2A2* and mouse *Btn2a2* SXY modules are aligned with that of *HLA-DRA*. Conserved positions are in bold. (D) The occupation of *HLA-DRA* and *BTN2A2* promoters by RFX and CIITA was quantified by ChIP in WT (Raji), *CIITA*^{-/-} (RJ2.2.5), and *RFX5*^{-/-} (SJO) B cells, or in untreated and IFN- γ -induced Me67.8 cells. Occupancy is expressed relative to WT or induced cells. (E, left) *BTN2A2* and *HLA-DRA* mRNAs were quantified by qRT-PCR in Raji (R), RJ2.2.5 (*CIITA*^{-/-}), RJ2.2.5 complemented with expression vectors encoding CIITA isoforms I, III, or IV, and *RFX5*-deficient B cell lines BLS-1 (B), Da (D), Ro, Abd (A), and 6.1.6 (6). (Right) *BTN2A2* and *HLA-DRA* mRNAs were quantified by qRT-PCR in untreated and IFN- γ -induced human umbilical vein endothelial cells (WT) and *CIITA*^{-/-} fibroblasts (BLS3). Results were normalized using *TBP* mRNA and expressed relative to Raji (left) or uninduced WT cells (right). (F) *Btn2a2* and *H2-Aa* mRNAs were quantified by qRT-PCR in splenic B cells, BMDCs, or untreated and IFN- γ -treated MEFs from WT, *CIITA*^{-/-}, and *RFX5*^{-/-} mice. Results were normalized using *TBP* mRNA or *18S* ribosomal RNA and expressed relative to WT. (G) *BTN2A2* expression by untreated and LPS-activated splenic CD19⁺ B cells from WT, *Btn2a2*^{-/-}, *Rfx5*^{-/-}, and *Clita*^{-/-} mice was analyzed by flow cytometry. (H) Luciferase reporter assays were performed in WT (Raji), *CIITA*^{-/-} (RJ2.2.5), and *RFX5*^{-/-} (SJO) cells using constructs driven by *HLA-DRA* (left) or *BTN2A2* (middle) promoters, or by a hybrid promoter in which the SXY module of *HLA-DRA* was replaced with that of *BTN2A2* (right). Activity is expressed relative to WT. (I) Luciferase activity was measured in WT (Raji) and *CIITA*^{-/-} (RJ2.2.5) cells for *BTN2A2-DRA* constructs containing mutations in the S, X, X2, and Y elements. Results are expressed relative to *HLA-DRA* in WT. (D–F, H, and I) Results show means and standard deviations derived from three experiments. (F and G) At least three mice per group were analyzed in each experiment.

Deregulated immune responses in *Btn2a2*^{-/-} mice are less severe than in mice lacking CTLA4 or PD1. CTLA4^{-/-} mice develop a severe lymphoproliferative disease leading to fatal multiorgan failure (Tivol et al., 1995; Waterhouse et al., 1995). PD1^{-/-} mice develop spontaneous autoimmune diseases (Nishimura et al., 1999, 2001). *Btn2a2*-deficient mice are rather more reminiscent of mice lacking PD1 ligands. Like *Btn2a2*^{-/-} mice, the latter exhibit increased T cell responses to antigen challenge but do not develop spontaneous autoimmunity (Latchman et al., 2004; Shin et al., 2005; Zhang et al., 2006).

***Btn2a2* deficiency potentiates antitumor vaccination**

The growth of B16-OVA tumors was impaired in OVA-immunized *Btn2a2*^{-/-} mice (Fig. 4 A). This correlated with increased tumor infiltration by conventional DCs, CD4⁺IFN- γ ⁺ T cells, CD4⁺IFN- γ ⁺IL-17⁺ T cells, and CD8⁺IFN- γ ⁺ T cells. There was no change in CD4⁺IL-17⁺ or CD4⁺Foxp3⁺ T cells (Fig. 4 B). This is consistent with the fact that IFN- γ -producing T cells are critical for controlling B16-OVA tumors (Muranski et al., 2008).

The benefit of targeting co-inhibitory pathways has recently been highlighted by unprecedented successes in cancer immunotherapy using biologics targeting the CTLA4 and PD1 axes (Azijli et al., 2014; Cohen, 2014). Identification of BTN2A2 as a new co-inhibitory molecule paves the way for exploring its potential value as a novel therapeutic target for cancer.

MATERIALS AND METHODS

Scan for SXY modules. The human genome was scanned as described previously (Krawczyk et al., 2007) to identify promoters containing regions with strong homology to the consensus SXY module of MHCII genes.

Quantitative RT-PCR (qRT-PCR). qRT-PCR was performed using the iCycler iQ Real-Time PCR Detection system (Bio-Rad Laboratories) and a SYBR green-based kit (iQ Supermix; Bio-Rad Laboratories). Amplification specificity was controlled by gel electrophoresis and melting curve analysis. Results were quantified using a standard curve generated with serial dilutions of a control cDNA. Amplifications were performed in triplicate. Expression was normalized using *TBP* mRNA or *18S* ribosomal RNA.

ChIP. Quantitative ChIP experiments using anti-RFX5 and anti-CIITA Ab's were performed as previously described (Krawczyk et al., 2007).

Luciferase reporter gene assays. The pDRApprox vector has been previously described (Krawczyk et al., 2007). This vector contains an *HLA-DRA* promoter fragment (from -151 to +10) inserted upstream of the firefly luciferase reporter gene in the pGL3b vector (Promega). The vector containing the *BTN2A2* promoter was generated by inserting a PCR-amplified fragment encompassing the SXY module and transcription start site of *BTN2A2* between the MluI and BglII sites of pGL3b. Vectors containing hybrid promoters were generated by replacing the *HLA-DRA* SXY module with *BTN* SXY fragments using the MluI-BglII sites in pDRApprox. Mutations were introduced as previously described (Krawczyk et al., 2007). Raji, RJ2.2.5, and SJO cells were cotransfected with the firefly luciferase reporter vectors and a control renilla luciferase vector. Transfections were performed by electroporation (950 μ F and 0.21 V). Dual luciferase assays were performed as previously described (Krawczyk et al., 2007).

Cell lines. The WT human B cell line Raji, human melanoma cell line Me67.8, CIITA-deficient human B cell mutant RJ2.2.5, RFXAP-deficient human B cell mutant 6.1.6, RFX-deficient B cell lines established from MHCII deficiency patients (Da, Ro, Ab, SJO, and BLS1), and a CIITA-deficient fibroblast line established from an MHCII-deficient patient (BLS3) have been previously described (Reith et al., 2005). Human cell lines were grown in an RPMI + Glutamax medium (Invitrogen) supplemented with 10–15% FCS and antibiotics. Me67.8 and BLS3 cells were induced with 200 U/ml of human IFN- γ (Invitrogen). The A20 mouse B cell line (ATCC) was cultured in an RPMI + Glutamax medium supplemented with 10% FCS, 0.1% β -mercaptoethanol, and antibiotics.

Primary cells. Human umbilical vein endothelial cells were induced with 1,000 U/ml of human IFN- γ . MEFs were isolated from mice at embryonic day 14, filtered through a cell strainer, and plated in tissue culture dishes. MEFs were induced with 100 U/ml of mouse IFN- γ (Invitrogen). Splenic mouse B cells were purified by sorting CD19⁺ cells with magnetic beads (Miltenyi Biotec) using autoMACS (Miltenyi Biotec) or by sorting B220⁺ cells using FACS Vantage (BD). Mouse BMDCs were derived by culturing 10⁶ BM cells/ml in DMEM supplemented with GM-CSF for 6–8 d and then purified by sorting CD11c^{high} cells using FACS Vantage.

in dLNs of WT and *Btn2a2*^{-/-} (KO) mice immunized with OVA₁ peptide plus CpG. Results were pooled from two experiments, each with three to five mice per group. (G and H) CD4⁺ T cells from *Btn2a2*^{-/-} (KO) and WT mice were activated with anti-CD3 or anti-CD3/anti-CD28 in the absence or presence of a BTN2A2-Fc fusion protein or control c-Myc Ab. Proliferation (Ki67 expression), activation (CD25 expression), and T_{reg} differentiation (Foxp3 expression) were assessed by flow cytometry (G). ELISA was used to quantify IFN- γ production (H). (I) CD8⁺ T cells from *Btn2a2*^{-/-} (KO) and WT mice were activated with anti-CD3 in the presence or absence of a BTN2A2-Fc fusion protein or control c-Myc Ab. Activation (CD25 and CD69 expression) was assessed by flow cytometry. (G–I) Results are representative of three experiments, each with three mice per group. (B–I) *, P < 0.05; **, P < 0.01; ***, P < 0.001; ****, P < 0.0001. Error bars are standard deviation of the mean.

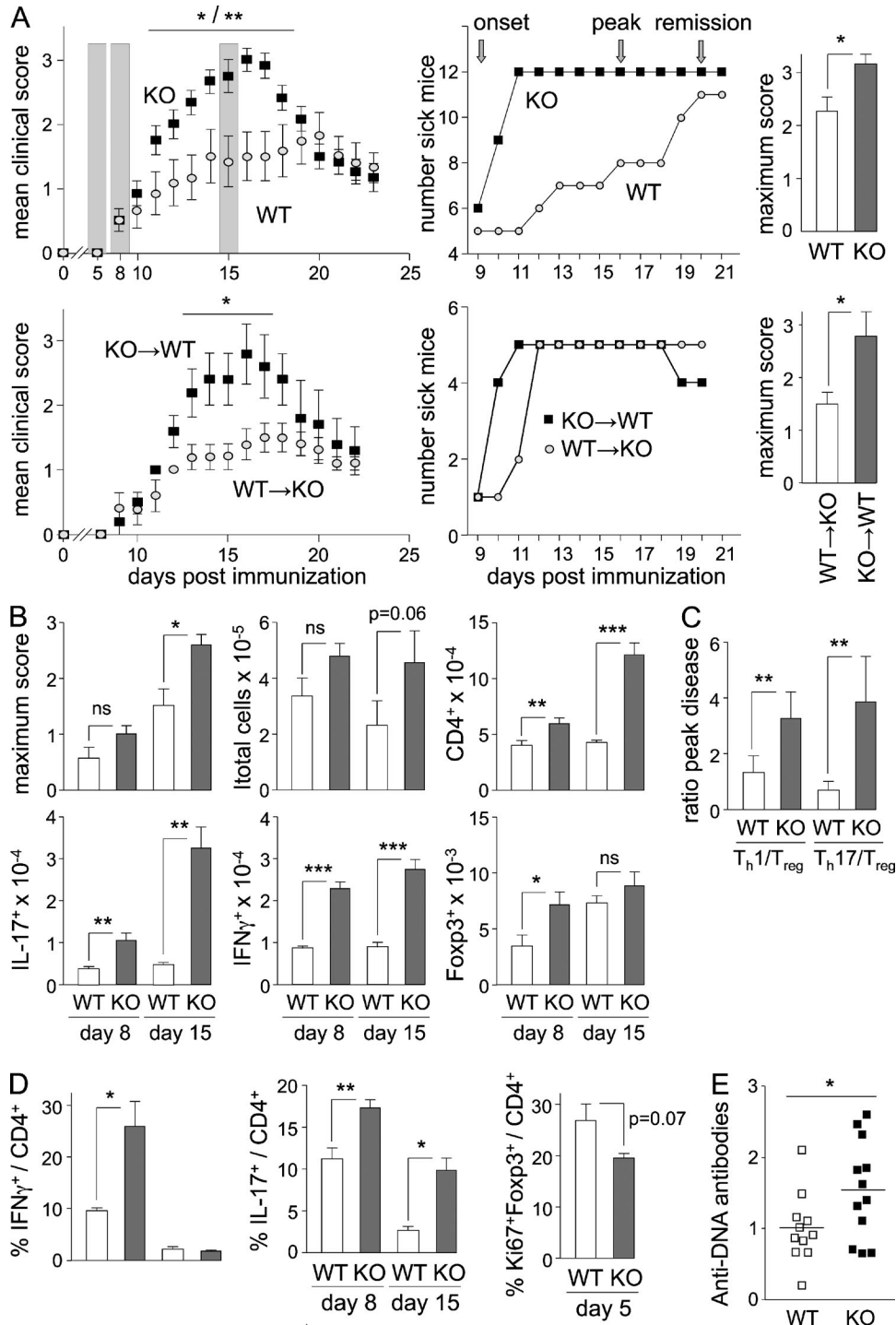


Figure 3. **Autoimmunity in *Btn2a2*^{-/-} mice.** (A) EAE was induced by immunization with MOG₃₅₋₅₅ + CFA in *Btn2a2*^{-/-} (KO) and WT mice or in KO→WT and WT→KO chimeras. Mean clinical scores, disease incidence, and maximum scores are shown. Shading (top left graph) indicates time points analyzed in B and C. (B) Maximum disease scores and SC-infiltrating cells (total cells, CD4⁺ T cells, and MOG-specific IFN- γ ⁺, IL-17⁺, or Foxp3⁺ CD4⁺ T cells) were quantified by flow cytometry in WT and *Btn2a2*^{-/-} mice at disease onset and peak disease. (C) Ratios between SC-infiltrating Th1 or Th17 cells and T_{reg} cells were determined at peak disease in WT and *Btn2a2*^{-/-} mice. (A–C) Results are pooled from two experiments, each with five mice per group. (D) IFN- γ ⁺, IL-17⁺, and Ki67⁺Foxp3⁺ CD4⁺ T cells were quantified by flow cytometry in LN cells harvested at pre-onset, onset, and peak disease. Results are derived from three experiments, each with six mice per group. (E) Serum anti-DNA Ab titers were measured by ELISA in age-matched 1-yr-old *Btn2a2*^{-/-} and WT mice. A representative of two experiments is shown, each with eight mice per group. *, P < 0.05; **, P < 0.01; ***, P < 0.001; ns, not significant. Error bars are standard deviation of the mean.

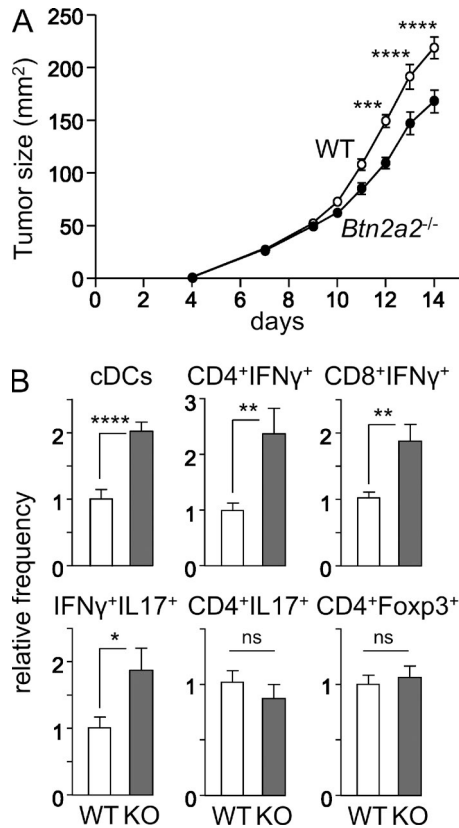


Figure 4. Impaired tumor growth in *Btn2a2*^{-/-} mice. (A) B16-OVA tumor growth was assessed in OVA-immunized WT and *Btn2a2*^{-/-} mice. (B) Tumor-infiltrating conventional DCs and CD4⁺IFN- γ ⁺, CD8⁺IFN- γ ⁺, CD4⁺IFN- γ ⁺IL-17⁺, CD4⁺IL-17⁺, and CD4⁺Foxp3⁺ T cells were quantified by flow cytometry. Results are pooled from two experiments, each with six mice per group, and expressed relative to WT. *, $P < 0.05$; **, $P < 0.01$; ***, $P < 0.001$; ****, $P < 0.0001$; ns, not significant. Error bars are standard deviation of the mean.

BTN2A2 protein expression. Mouse splenic CD19⁺ B cells were cultured with or without 100 ng/ml LPS for 18 h in RPMI 1640 containing 10% FCS, 100 U/ml penicillin, 100 U/ml streptomycin, and 50 μ M 2-ME. Cells were harvested and preblocked with Fc Block (BD). Cells were stained with human mAb's against mouse 1 μ g/ml BTN2A2 (Novimmune SA) and anti-human IgG (SouthernBiotech).

Generation of *Btn2a2*^{-/-} mice. The targeting strategy was designed to permit conditional deletion of a region encompassing the promoter (including the SXY module), the transcription start site and first noncoding exon, and the second exon containing the translation initiation codon and leader sequence (Fig. 2 A). The targeting construct contained a long region of homology (~5.5 kb) situated upstream of the promoter, the region to be deleted (~1.2-kb segment spanning the promoter and first two exons) flanked (floxed) by loxP sites, a neomycin resistance cassette (Pgk-neo) flanked by Frt sites, and a short region of homology (~2.5 kb) situated

within the body of the gene. This construct was used to generate *Btn2a2*-targeted mice (Taconic). The targeting vector was electroporated into C57BL/6 Ntac embryonic stem (ES) cells. G418-resistant ES cell clones were screened to identify homologous recombinants by Southern blotting using 5' and 3' probes situated outside of the targeting vector. The absence of nonhomologous insertions was verified by Southern blotting with a probe for the neomycin resistance gene. Injection of ES cells into blastocysts and blastocyst implantation were performed according to standard procedures. Chimeric mice were bred directly with FLP deleter mice (C57BL/6-Tg(*ACTB-Flpe*)2arte) to obtain germline transmission of the targeted allele and deletion of the Frt-flanked neomycin resistance cassette. Germline transmission of the targeted allele lacking the neomycin resistance cassette was confirmed by PCR. Deletion of the loxP-flanked (floxed) segment of the targeted *Btn2a2* allele was achieved by crossing with cre deleter mice (C57BL/6-Gt(*ROSA*)26Sor^{tm16(cre)Arte}). Deletion of the loxP-flanked (floxed) segment was confirmed by PCR.

Ab's and flow cytometry. Ab's for cell purification and flow cytometry were as follows: CD16/CD32 (Fc Block; BD), TCR V α 2 (BioLegend), CD4 (BioLegend), CD25 (BioLegend), CD69 (BioLegend), CD19 (BioLegend), Foxp3 (BD), IL-17A (BD), IFN- γ (BD), Ki67 (BD), TCR γ δ (BioLegend), NK-1.1 (BioLegend), CD49b (BioLegend), CD8a (BioLegend), CD11c (BioLegend), Siglec H (BioLegend), PDCA-1 (BioLegend), B220 (BioLegend), IL-5 (BD), IFN- γ (BD), CD28 (Bioscience), CD3 (eBioscience), and anti-human IgG-Fc (SouthernBiotech). Intracellular cytokine staining was done with the Cytofix/Cytoperm kit (BD). T cell proliferation was assessed by flow cytometry using an anti-human Ki67 staining kit (BD). Foxp3 staining was performed with an eBioscience kit. Flow cytometry was performed with FACS CyAn (Beckman Coulter) and analyzed with FlowJo software.

Mice. OTII, OTI, *RFX5*^{-/-}, and *CIIIta*^{-/-} mice have been previously described (Hogquist et al., 1994; Chang et al., 1996; Barnden et al., 1998; Clausen et al., 1998). Mice were on a C57BL/6 background, maintained under specific pathogen-free conditions, and sacrificed at 6–10 wk. Experiments were performed in accordance with the cantonal and federal veterinary authorities.

BM chimeras. BM from tibia and femurs was recovered by flushing with PBS-EDTA and dissociated by passages through 20-gauge needles. 5×10^6 cells were injected i.v. into irradiated (950 rad) recipients.

In vivo OTII and OTI cell activation. 6–10-wk-old mice were injected s.c. with 2 μ g/mouse OVA_{II} (OVA_{323–339}) or OVA_I (OVA_{257–264}) peptides and 5 nM CpG-B. After 24 h, $3–5 \times 10^6$ CD4⁺ OTII stained with CFSE (Invitrogen), or left unstained, were injected i.v. 4 d later, and dLN and nondraining LN cells were restimulated with 50 ng/ml PMA

(Sigma-Aldrich), 1 $\mu\text{g}/\text{ml}$ ionomycin (Sigma-Aldrich), and 1 $\mu\text{g}/\text{ml}$ GolgiPlug (BD) for 4 h at 37°C.

BTN2A2-Fc fusion protein. Fc fusion proteins were prepared by cloning a PCR-amplified cDNA fragment encoding aa 1–234 of mouse BTN2A2 into a pEAK8 vector containing a human IgG1 Fc tag. Peak cell lines were generated by transfection with Lipofectamine 2000 and selected by puromycin. Secreted Fc fusion proteins were purified on protein A Sepharose columns (GE Healthcare) by the AKTA Prime chromatography system. Purified protein was analyzed by gel electrophoresis, pooled, and desalted against PBS on PD-10 columns (GE Healthcare).

Effect of BTN2A2-Fc on in vitro T cell activation. CD4⁺ and CD8⁺ T cells from naive C57BL/6 and *Btn2a2*^{-/-} mice were purified to 95–98% purity using CD4⁺ or CD8⁺ T cell isolation kits (Miltenyi Biotec). Nunc maxisorp 96-well plates were coated with 2 $\mu\text{g}/\text{ml}$ anti-CD3 mAb and 10 $\mu\text{g}/\text{ml}$ Fc fusion proteins in PBS overnight at 4°C. Wells were washed three times with PBS, and 2×10^5 T cells were added per well in 200 μl RPMI 1640 containing 10% FCS, 100 U/ml penicillin, 100 U/ml streptomycin, and 50 μM 2-ME, with or without 2 $\mu\text{g}/\text{ml}$ anti-CD28 Ab. Activation was assessed by flow cytometry after 12 h (CD69 staining) and 96 h (CD25 staining). Proliferation (Ki67 staining) was assessed by flow cytometry after 72 or 96 h. CD4⁺Foxp3⁺ T_{reg} cells were quantified by flow cytometry after 96 h. Th1 cell development was assessed by quantifying IFN- γ production by ELISA.

Immunization. Mice were immunized twice, 2 wk apart, by s.c. injection of 10 μg endotoxin-free OVA (Hyglos) adsorbed to 250 μg aluminum hydroxide or, when indicated, after the addition of 50 μg CpG-B (Eurofins MWG Operon).

Quantification of IFN- γ - and IL-5-producing OVA-specific T cells. Single-cell suspensions from spleens of immunized mice were suspended in DMEM (2% FCS; Gibco). 90% of the suspensions were collected after allowing debris, fat, and red blood cells to settle at 4°C for 10 min. Multiscreen hemagglutinin nitrocellulose-bottomed plates (EMD Millipore) were coated overnight at 37°C with anti-IFN- γ or anti-IL-5 Ab's, washed with PBS (0.1% Tween 20), blocked with DMEM (10% FCS), and incubated for 48 h at 37°C with serial dilutions of the single-cell suspensions, with or without OVA. Plates were then incubated with biotinylated anti-IFN- γ or anti-IL-5 Ab's, incubated for 2 h at room temperature (RT), washed, and incubated for 2 h at RT with extravidin peroxidase (Sigma-Aldrich). After washing, substrate was added and reactions were stopped after 12 min at RT in the dark by rinsing with water. Wells containing spots were counted by eye. OVA-specific IFN- γ - or IL-5-producing cells were quantified by subtracting the numbers of cells counted in the absence of OVA.

Quantification of IFN- γ and IL-5 secretion by OVA-specific T cells. Single-cell suspensions from spleens of immunized mice were suspended in DMEM (2% FCS; Gibco), and 90% of the suspension was collected after allowing debris, fat, and red blood cells to settle at 4°C for 10 min. Cell suspensions were restimulated with OVA, and supernatants were collected after 72 h. Secreted cytokines were quantified by ELISA. Maxisorp plates (Nunc) were coated overnight at 4°C with anti-IFN- γ or anti-IL-5 Ab's (BD), blocked for 2 h at RT with PBS (0.05% Tween 20 and 1% BSA), incubated overnight at 4°C with serial supernatant dilution, washed, incubated for 2 h at RT with biotinylated anti-IFN- γ or anti-IL-5 Ab's, washed, incubated for 45 min at RT with extravidin peroxidase (Sigma-Aldrich), and washed, and the OD was read after incubation with substrate for 2 h at RT.

Antitumor vaccination. Mice were immunized s.c. with 5 mmol CpG-B and 10 μg OVA_{II} 7 d before the transplantation of 0.5×10^6 B16-OVA cells cultured at 70% confluence. Tumor size (length multiplied by width) was measured with a caliper every 1–2 d. For tumor-infiltrating lymphocyte analysis, tumors were digested with 1 mg/ml collagenase D and 10 $\mu\text{g}/\text{ml}$ DNase I. Tumor-infiltrating lymphocytes were enriched using lymphocyte M solution (Cedarlane Laboratories), incubated for 4 h with 50 ng/ml PMA, 1 $\mu\text{g}/\text{ml}$ ionomycin, and 1 $\mu\text{g}/\text{ml}$ GolgiPlug, and analyzed by flow cytometry.

EAE. Mice were injected s.c. in both flanks with 100 μg MOG peptide (MOG_{35–55}; Anawa) in 200 μl PBS/CFA (1:1; Difco) and injected i.v. on days 0 and 2 with 100 ng pertussis toxin (Sigma-Aldrich). EAE scoring was as follows: 1, flaccid tail; 2, impaired righting reflex and hind limb weakness; 3, partial hind limb paralysis; 4, complete hind limb paralysis; 5, hind limb paralysis with partial fore limb paralysis; 6, moribund. Mice were sacrificed above a score of 4.

SC infiltration. SCs of animals perfused with HBSS were minced with a scalpel blade and digested 1 h at 37°C in HBSS, 1 mg/ml DNase I (Roche), and 1 mg/ml collagenase D (Roche). Digestions were quenched on ice with 50% FCS and passed through 70 μm nylon cell strainers (Falcon; BD). Suspensions were pelleted, suspended in 30% Percoll (Sigma-Aldrich), underlayered with 70% Percoll in HBSS, and centrifuged at 1,000 g for 20 min at RT without brakes. Myelin was removed by aspiration. The interphase plus ~80% of the 30% Percoll were collected, diluted at least threefold with HBSS, and centrifuged at 300 g. Cells were washed twice more and used for restimulation for 24 h with MOG_{35–55}. GolgiPlug was added for the last 4 h. Cells were analyzed by flow cytometry.

Anti-DNA Ab titers in aged *Btn2a2*^{-/-} mice. ELISA was used to determine serum titers of autoantibodies against double-stranded DNA. Double-stranded DNA was coated onto ELISA plates precoated with poly-L-lysine (Sigma-Aldrich). Plates were in-

cubated with diluted serum samples, and assays were developed with alkaline phosphatase-conjugated goat anti-mouse IgG (SouthernBiotech). Results are expressed in units per milliliter based on a standard curve derived from pooled sera from normal mice or MRL-Fas^{lpr} mice.

Statistics. Unpaired nonparametric Mann-Whitney or two-way ANOVA tests were used to assess statistical significance in tumor growth experiments. Two-tailed Student's *t* tests were used in all other experiments.

ACKNOWLEDGMENTS

We are grateful to all members of our laboratories for helpful discussions.

Work in the laboratory of W. Reith was supported by the Swiss National Science Foundation (grant 310030B_144085), the Geneva Cancer League, the Swiss Cancer League, and the Swiss Multiple Sclerosis Society.

The authors declare no competing financial interests.

Submitted: 10 March 2015

Accepted: 10 December 2015

REFERENCES

- Afrache, H., P. Gouret, S. Ainouche, P. Pontarotti, and D. Olive. 2012. The butyrophilin (BTN) gene family: from milk fat to the regulation of the immune response. *Immunogenetics*. 64:781–794. <http://dx.doi.org/10.1007/s00251-012-0619-z>
- Ammann, J.U., A. Cooke, and J. Trowsdale. 2013. Butyrophilin Btn2a2 inhibits TCR activation and phosphatidylinositol 3-kinase/Akt pathway signaling and induces Foxp3 expression in T lymphocytes. *J. Immunol.* 190:5030–5036. <http://dx.doi.org/10.4049/jimmunol.1203325>
- Arnett, H.A., and J.L. Viney. 2014. Immune modulation by butyrophilins. *Nat. Rev. Immunol.* 14:559–569. <http://dx.doi.org/10.1038/nri3715>
- Arnett, H.A., S.S. Escobar, E. Gonzalez-Suarez, A.L. Budelsky, L.A. Steffen, N. Boiani, M. Zhang, G. Siu, A.W. Brewer, and J.L. Viney. 2007. BTN2L2, a butyrophilin/B7-like molecule, is a negative costimulatory molecule modulated in intestinal inflammation. *J. Immunol.* 178:1523–1533. <http://dx.doi.org/10.4049/jimmunol.178.3.1523>
- Aziji, K., E. Stelloo, G.J. Peters, and A.J. VAN DEN Eertwegh. 2014. New developments in the treatment of metastatic melanoma: immune checkpoint inhibitors and targeted therapies. *Anticancer Res.* 34:1493–1505.
- Barnden, M.J., J. Allison, W.R. Heath, and F.R. Carbone. 1998. Defective TCR expression in transgenic mice constructed using cDNA-based α - and β -chain genes under the control of heterologous regulatory elements. *Immunol. Cell Biol.* 76:34–40. <http://dx.doi.org/10.1046/j.1440-1711.1998.00709.x>
- Boyden, L.M., J.M. Lewis, S.D. Barbee, A. Bas, M. Girardi, A.C. Hayday, R.E. Tigelaar, and R.P. Lifton. 2008. Skint1, the prototype of a newly identified immunoglobulin superfamily gene cluster, positively selects epidermal $\gamma\delta$ T cells. *Nat. Genet.* 40:656–662. <http://dx.doi.org/10.1038/ng.108>
- Chang, C.H., S. Guerder, S.C. Hong, W. van Ewijk, and R.A. Flavell. 1996. Mice lacking the MHC class II transactivator (CIITA) show tissue-specific impairment of MHC class II expression. *Immunity*. 4:167–178. [http://dx.doi.org/10.1016/S1074-7613\(00\)80681-0](http://dx.doi.org/10.1016/S1074-7613(00)80681-0)
- Clausen, B.E., J.M. Waldhuber, F. Schwenk, E. Barras, B. Mach, K. Rajewsky, I. Förster, and W. Reith. 1998. Residual MHC class II expression on mature dendritic cells and activated B cells in RFX5-deficient mice. *Immunity*. 8:143–155. [http://dx.doi.org/10.1016/S1074-7613\(00\)80467-7](http://dx.doi.org/10.1016/S1074-7613(00)80467-7)
- Cohen, I.R. 2014. Activation of benign autoimmunity as both tumor and autoimmune disease immunotherapy: a comprehensive review. *J. Autoimmun.* 54:112–117. <http://dx.doi.org/10.1016/j.jaut.2014.05.002>
- Hogquist, K.A., S.C. Jameson, W.R. Heath, J.L. Howard, M.J. Bevan, and F.R. Carbone. 1994. T cell receptor antagonist peptides induce positive selection. *Cell*. 76:17–27. [http://dx.doi.org/10.1016/0092-8674\(94\)90169-4](http://dx.doi.org/10.1016/0092-8674(94)90169-4)
- Krawczyk, M., E. Leimgruber, Q. Seguí-Estévez, I. Dunand-Sauthier, E. Barras, and W. Reith. 2007. Expression of RAB4B, a protein governing endocytic recycling, is co-regulated with MHC class II genes. *Nucleic Acids Res.* 35:595–605. <http://dx.doi.org/10.1093/nar/gkl980>
- Krawczyk, M., Q. Seguí-Estévez, E. Leimgruber, P. Sperisen, C. Schmid, P. Bucher, and W. Reith. 2008. Identification of CIITA regulated genetic module dedicated for antigen presentation. *PLoS Genet.* 4:e1000058. <http://dx.doi.org/10.1371/journal.pgen.1000058>
- Latchman, Y.E., S.C. Liang, Y. Wu, T. Chernova, R.A. Sobel, M. Klemm, V.K. Kuchroo, G.J. Freeman, and A.H. Sharpe. 2004. PD-L1-deficient mice show that PD-L1 on T cells, antigen-presenting cells, and host tissues negatively regulates T cells. *Proc. Natl. Acad. Sci. USA.* 101:10691–10696. <http://dx.doi.org/10.1073/pnas.0307252101>
- Malcherek, G., L. Mayr, P. Roda-Navarro, D. Rhodes, N. Miller, and J. Trowsdale. 2007. The B7 homolog butyrophilin BTN2A1 is a novel ligand for DC-SIGN. *J. Immunol.* 179:3804–3811. <http://dx.doi.org/10.4049/jimmunol.179.6.3804>
- Muranski, P., A. Boni, P.A. Antony, L. Cassard, K.R. Irvine, A. Kaiser, C.M. Paulos, D.C. Palmer, C.E. Touloukian, K. Ptak, et al. 2008. Tumor-specific Th17-polarized cells eradicate large established melanoma. *Blood*. 112:362–373. <http://dx.doi.org/10.1182/blood-2007-11-120998>
- Nishimura, H., M. Nose, H. Hiai, N. Minato, and T. Honjo. 1999. Development of lupus-like autoimmune diseases by disruption of the PD-1 gene encoding an ITIM motif-carrying immunoreceptor. *Immunity*. 11:141–151. [http://dx.doi.org/10.1016/S1074-7613\(00\)80089-8](http://dx.doi.org/10.1016/S1074-7613(00)80089-8)
- Nishimura, H., T. Okazaki, Y. Tanaka, K. Nakatani, M. Hara, A. Matsumori, S. Sasayama, A. Mizoguchi, H. Hiai, N. Minato, and T. Honjo. 2001. Autoimmune dilated cardiomyopathy in PD-1 receptor-deficient mice. *Science*. 291:319–322. <http://dx.doi.org/10.1126/science.291.5502.319>
- Ogg, S.L., A.K. Weldon, L. Dobbie, A.J. Smith, and I.H. Mather. 2004. Expression of butyrophilin (Bt1a1) in lactating mammary gland is essential for the regulated secretion of milk-lipid droplets. *Proc. Natl. Acad. Sci. USA.* 101:10084–10089. <http://dx.doi.org/10.1073/pnas.0402930101>
- Reith, W., S. LeibundGut-Landmann, and J.M. Waldhuber. 2005. Regulation of MHC class II gene expression by the class II transactivator. *Nat. Rev. Immunol.* 5:793–806. <http://dx.doi.org/10.1038/nri1708>
- Sandstrom, A., C.M. Peigné, A. Léger, J.E. Crooks, F. Konczak, M.C. Gesnel, R. Breathnach, M. Bonneville, E. Scotet, and E.J. Adams. 2014. The intracellular B30.2 domain of butyrophilin 3A1 binds phosphoantigens to mediate activation of human V γ 9V δ 2 T cells. *Immunity*. 40:490–500. <http://dx.doi.org/10.1016/j.immuni.2014.03.003>
- Shin, T., K. Yoshimura, T. Shin, E.B. Crafton, H. Tsuchiya, F. Housseau, H. Koseki, R.D. Schulick, L. Chen, and D.M. Pardoll. 2005. In vivo costimulatory role of B7-DC in tuning T helper cell 1 and cytotoxic T lymphocyte responses. *J. Exp. Med.* 201:1531–1541. <http://dx.doi.org/10.1084/jem.20050072>
- Smith, I.A., B.R. Knezevic, J.U. Ammann, D.A. Rhodes, D. Aw, D.B. Palmer, I.H. Mather, and J. Trowsdale. 2010. BTN1A1, the mammary gland butyrophilin, and BTN2A2 are both inhibitors of T cell activation. *J. Immunol.* 184:3514–3525. <http://dx.doi.org/10.4049/jimmunol.0900416>
- Swanson, R.M., M.A. Gavin, S.S. Escobar, J.B. Rottman, B.P. Lipsky, S. Dube, L. Li, J. Bigler, M. Wolfson, H.A. Arnett, and J.L. Viney. 2013. Butyrophilin-like 2 modulates B7 costimulation to induce Foxp3 expression and

- regulatory T cell development in mature T cells. *J. Immunol.* 190:2027–2035. <http://dx.doi.org/10.4049/jimmunol.1201760>
- Tivol, E.A., F. Borriello, A.N. Schweitzer, W.P. Lynch, J.A. Bluestone, and A.H. Sharpe. 1995. Loss of CTLA-4 leads to massive lymphoproliferation and fatal multiorgan tissue destruction, revealing a critical negative regulatory role of CTLA-4. *Immunity.* 3:541–547. [http://dx.doi.org/10.1016/1074-7613\(95\)90125-6](http://dx.doi.org/10.1016/1074-7613(95)90125-6)
- Vavassori, S., A. Kumar, G.S. Wan, G.S. Ramanjaneyulu, M. Cavallari, S. El Daker, T. Beddoe, A. Theodossis, N.K. Williams, E. Gostick, et al. 2013. Butyrophilin 3A1 binds phosphorylated antigens and stimulates human $\gamma\delta$ T cells. *Nat. Immunol.* 14:908–916. <http://dx.doi.org/10.1038/ni.2665>
- Viken, M.K., A. Blomhoff, M. Olsson, H.E. Akselsen, F. Pociot, J. Nerup, I. Kockum, A. Cambon-Thomsen, E. Thorsby, D.E. Undlien, and B.A. Lie. 2009. Reproducible association with type 1 diabetes in the extended class I region of the major histocompatibility complex. *Genes Immun.* 10:323–333. <http://dx.doi.org/10.1038/gene.2009.13>
- Waterhouse, P., J.M. Penninger, E. Timms, A. Wakeham, A. Shahinian, K.P. Lee, C.B. Thompson, H. Griesser, and T.W. Mak. 1995. Lymphoproliferative disorders with early lethality in mice deficient in Ctl α -4. *Science.* 270:985–988. <http://dx.doi.org/10.1126/science.270.5238.985>
- Yamazaki, T., I. Goya, D. Graf, S. Craig, N. Martin-Orozco, and C. Dong. 2010. A butyrophilin family member critically inhibits T cell activation. *J. Immunol.* 185:5907–5914. <http://dx.doi.org/10.4049/jimmunol.1000835>
- Zhang, Y., Y. Chung, C. Bishop, B. Daugherty, H. Chute, P. Holst, C. Kurahara, F. Lott, N. Sun, A.A. Welcher, and C. Dong. 2006. Regulation of T cell activation and tolerance by PDL2. *Proc. Natl. Acad. Sci. USA.* 103:11695–11700. <http://dx.doi.org/10.1073/pnas.0601347103>